Ouyang PC, Chung KW, Fathauer RW *et al.* Generation of Escher-like rosette drawings. JOURNAL OF COMPUTER SCIENCE AND TECHNOLOGY 39(6): 1466-1479 Nov. 2024. DOI: 10.1007/s11390-024-2874-5

Generation of Escher-Like Rosette Drawings

Pei-Chang Ouyang[1] (欧阳培昌), Kwok-Wai Chung[2], Robert W. Fathauer[3], Alain Nicolas[4]
Jian-Hua Pang[1] (庞建华), Shi-Yun Cao[1] (曹石云), and Krzysztof Gdawiec[5, *]

[1] *School of Science, Guangxi University of Science and Technology, Liuzhou 545006, China*

[2] *Department of Mathematics, City University of Hong Kong, Hong Kong, China*

[3] *Tessellations Company, 3913 E. Bronco Trail, Phoenix AZ 85044, U.S.A.*

[4] *Nicolas Tessellation, 15 rue Georges Auric, Quincy-sous-Sénart 91480, France*

[5] *Institute of Computer Science, University of Silesia, Bedzinska 39, Sosnowiec 41-200, Poland*

E-mail: 10002367@gxust.edu.cn; makchung@cityu.edu.hk; tessellations@cox.net; al.nicolas15@gmail.com
100001019@gxust.edu.cn; sycao@gxust.edu.cn; krzysztof.gdawiec@us.edu.pl

Received November 19, 2022; accepted August 30, 2024.

Abstract *"Smaller and Smaller"* is a woodcut by the Dutch artist M.C. Escher in which the lizards designed in a rosette tiling approach the centre by geometric series. This paper proposes an easy method to generate drawings similar to *"Smaller and Smaller"*. To this end, the geometrical structure of rosette tilings is first considered from the viewpoint of the symmetry group in detail. This gives a simple way to construct rosette tilings. Then, a one-to-one mapping between kite-shaped and square regions is presented to embed a pre-designed template into kite-shaped tiles of rosette tilings. Next, the algorithms for rendering the rosette tilings are discussed. Finally, some detailed implements of producing rosette drawings are specified. The presented examples show that by using the existing rich wallpaper templates, the method proposed in the paper can generate a variety of Escher-like rosette drawings.

Keywords color symmetry, Escher art, rosette tiling, spiral symmetry

1 Introduction

With the development of computer graphics technology, there is considerable research on the generation of aesthetic patterns based on mathematical principles. This includes not only the well-known fractals[1, 2] but also patterns of the wallpaper[3–5], cyclic and/or dihedral[3, 6], hyperbolic[7, 8], and spiral[1, 9, 10] symmetries. However, the visual appeal of computer-generated patterns mainly comes from harmonious and graceful symmetries. A major defect of such patterns is that they lack artistic vitality.

Dutch artist M.C. Escher is a great graphic artist. The order, rigour, and accuracy of mathematics formed the soul of his work and became his unique classic sign. He showed that seemingly contradictory sensibility and reason could be perfectly integrated[11], which makes a durable and profound influence on both artists and scientific researchers. Due to the aesthetic appeal as well as commercial potential, there appear a lot of studies dedicated to the creation of Escher-like arts[11], such as Escherization[12, 13], Escher Spheres[14], metamorphosis[15], fractal drawings[16], Escher transmutation[17, 18], and hyperbolic drawings[19, 20]. The most striking feature of the above research is that the motifs are well recognizable.

As a common and beautiful curve in nature, the logarithmic spiral has been explored extensively by Escher, including "Development II" (1939), "Whirlpools" (1957), "Path of Life I" (1958), "Path of Life II"

Regular Paper

This work was supported by the Base and Talent Project of Science and Technology of Guangxi Zhuang Autonomous Region of China under Grant Nos. AA21196008 and 2024AC45008, the Guangxi Natural Science Foundation under Grant No. 2024GXNSFAA010507, the Natural Science Foundation of China under Grant Nos. 62462004 and 62062042, the Doctor Startup Foundation of Guangxi University of Science and Technology under Grant No. 21Z48, and the Philosophy and Social Science Research Foundation of Guangxi Zhuang Autonomous Region of China under Grant No. 23FWY025.

*Corresponding Author

(1958), and "Sphere Surface with Fish" (1958). There is an outstanding woodcut that has to be mentioned – *"Smaller and Smaller"*[①]. In this work, as the lizards of different colours approach the centre infinitely, they are progressively reduced by a geometric series, which conveys the elements of colour, spiral, similar, and cyclic symmetries simultaneously. In a letter to his son, Escher wrote, "*at moments of great enthusiasm it seems to me that no one in the world has ever made something this beautiful and important*".

Inspired by Escher's spiral artworks, rich programs[②, ③, ④] and studies[⑤, ⑥][21, 22] focus on creating spiral patterns. One of the types of spiral patterns is kite-based tiling[23] (see Fig.1(a) for an example of such tiling). In [23, 24], Fathauer studied only some properties of these tilings and has not introduced any method suitable for the generation and rendering of such tilings.

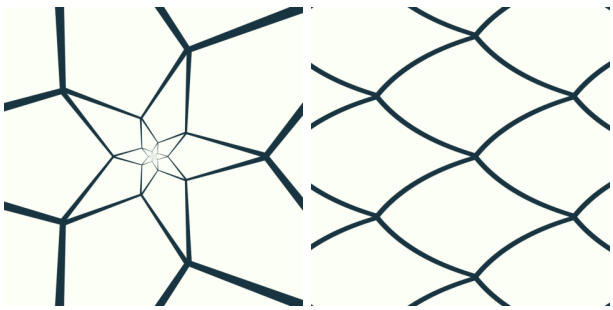

(a) (b)

Fig.1. (a) Kite-based tiling. (b) Periodic tiling that can be mapped to the tiling from (a) using the anti-Mercator mapping.

In the literature, we can find a description of one approach that could be used to render the kite-based tiling. The method is presented by Kaplan[⑤] and it is based on the use of anti-Mercator mapping[21]:

$$f(z) = e^z,$$

where $z \in \mathbb{C}$. In this method, we generate a periodic tiling, and then we transform it using the anti-Mercator mapping. Kaplan considered only periodic tilings in which the edges of the tiles are straight lines. When we transform such edges by the anti-Mercator mapping, then we get logarithmic spirals, concentric circles, or radial lines[⑤]. Therefore, we cannot get a rosette tiling in which all the edges are straight lines. To get the rosette tiling using the anti-Mercator mapping, we need to use a periodic tiling in which the edges are not straight lines (see Fig.1(b)), i.e., they are curves. Such a tiling was not reported in the literature earlier, therefore we would need to find its mathematical description. However, the approach of mapping this tiling with the anti-Mercator mapping has several drawbacks.

The edges of the periodic tiling are not straight lines, therefore it is harder to generate such tiling, and the control over the resulting kite-based tiling is not natural. To generate patterns in an Escher style, we need to embed some motif into the tiles of the periodic tiling. To do this, we can design the motif directly on the tile or create the motif in a square texture and next map it into the tile. In both cases, we need to take into account the fact that the anti-Mercator mapping will transform the motif; thus it needs to be properly designed. This is very difficult because of the non-linearity of the anti-Mercator mapping. Moreover, in the approach with the square texture, we need to calculate texture co-ordinates. Because the tiles in the periodic tiling have curved edges, it would require solving some non-linear equation, which can require the use of a numerical method and can be time-consuming.

Instead of finding the mathematical description of the tiling required in the anti-Mercator approach, in this paper, we propose some other method of generating rosette tilings that can be used to obtain drawings similar to Escher's *"Smaller and Smaller"*. This method will not have the mentioned drawbacks. The method is a direct one, i.e., we generate the tiling's kites directly, and the control over the tiling is natural by using two parameters. In the designing stage of the motif, we do not need to take into account any non-linear mapping because the motif will be directly mapped onto the kites. Moreover, the method is very simple to implement using shaders.

The remainder of this paper is outlined as follows. First, in Section 2, we introduce rosette tilings. We use the symmetry group to analyze its structure and describe how to construct rosette tilings in detail. Then, in Section 3, we establish a one-to-one map-

①https://mcescher.com/wp-content/uploads/2019/05/LW-413.jpg, Nov. 2024.
②https://tessellations.ca/2017/05/04/deforming-your-tessellations-into-infinite-spirals/, Nov. 2024.
③https://apps.apple.com/us/app/id534529876?platform=ipad, Nov. 2024.
④https://www.tissellator.com/, Nov. 2024.
⑤https://isohedral.ca/escher-like-spiral-tilings/, Nov. 2024.
⑥http://www.josleys.com/show_gallery.php?galid=290, Nov. 2024.

ping to deform a unit square into a kite-shaped region. Given a pre-designed wallpaper template, this technique allows us to embed the template into kite-shaped tiles of a rosette tiling. Next, we introduce the algorithms for rendering rosette tilings in Section 4 and present a gallery of the resulting Escher-like drawings in Section 5. To show the performance of the proposed rendering algorithm, in Section 6, we show the generation times of drawings obtained with the algorithm. Finally, we conclude the paper and show our future directions in Section 7.

2 Symmetry Group of Rosette Tiling

In this section, we introduce the rosette tiling of the symmetry, which is a combination of a rotational symmetry C_n with a self-similar radial scaling. We start by introducing some concepts about symmetry groups.

A symmetry of a tiling T is a transformation S under the action of which T is invariant. A tiling's symmetry group comprises all its symmetries. The elements $g_1, g_2, \ldots, g_n$ of a group G are called the set of generators if every element of G can be expressed as a finite product of their powers (including negative powers). The fundamental region F under the symmetry group G is a connected set whose transformed copies under the action of G cover the entire space without overlapping, except at the boundaries.

Fig.2(a) shows the type of the considered rosette tilings, which are tiled with similar kite-shaped tiles. The interweaving tiles make the tiling appear to be a complex structure. It is easy to check that it possesses similar and rotational symmetries. An easily overlooked fact is that this tiling also contains spiral symmetry, which is an important factor in why it conveys a strong visual appeal (see the dark–light red arm emphasized in Fig.2(b)). For convenience, we will use the complex numbers to handle the symmetries of rosette tiling and call the symmetry group associated with the tiling as the rosette group.

We first focus on the tile $ABCD$ marked in Fig.2(a). Assuming $\angle AOB = \pi/n$, $\angle DAB = \alpha$, and $\angle ABC = \theta$, by the Sine Rule, we obtain the ratio s of the short edge to the long edge as

$$s = \frac{|AD|}{|AB|} = \frac{\sin\dfrac{\theta}{2}}{\sin\left(\dfrac{\theta}{2} + \dfrac{\pi}{n}\right)}, \tag{1}$$

where $\theta = (n - 1/n)\pi - \alpha$. If we set $|BD| = 1$, then by the summation formula of geometric series, we get the coordinates $D = (s^2/(1 - s^2), 0)$. Then, the other vertices of the tile $ABCD$ can be easily calculated, obtaining:

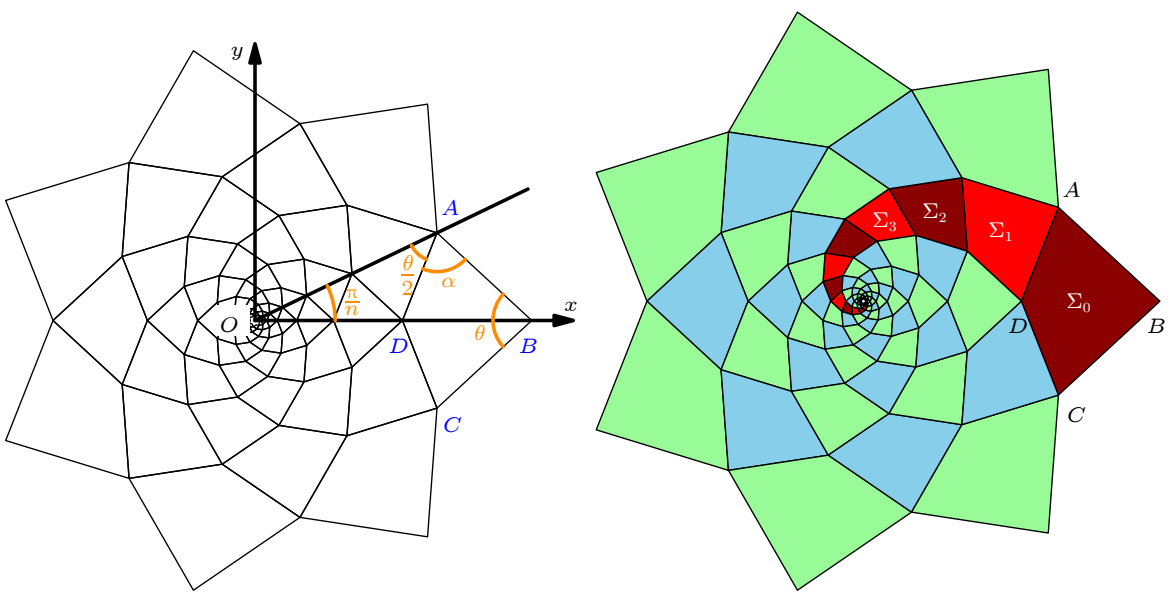

(a) (b)

Fig.2. (a) A rosette tiling by kite-shaped tiles centred at the origin of the Cartesian coordinate system. (b) A rosette tiling in which one arm is emphasized by the alternate dark and light red tiles. Vertices of the biggest tile in this arm are denoted by A, B, C, D and the tile itself is denoted by Σ_0. The arm is formed by tiles $\Sigma_k = g_2^k(\Sigma_0)$ for $k = 0, 1, 2, \ldots$. The tiles $T_{m,\,k}$ of the set $\{T_{m,\,k} | T_{m,\,k} = g_1^m[g_2^k(\Sigma_0)],\ m = 1, 2, 3, \ldots, n,\ k \in \mathbb{Z}\}$, cover the plane $\mathbb{C}^*$.

$$A = \left(\frac{s\cos\frac{\pi}{n}}{1-s^2}, \frac{s\cos\frac{\pi}{n}\tan\frac{\pi}{n}}{1-s^2} \right),$$
$$B = \left(\frac{1}{1-s^2}, 0 \right),$$
$$C = \left(\frac{s\cos\frac{\pi}{n}}{1-s^2}, -\frac{s\cos\frac{\pi}{n}\tan\frac{\pi}{n}}{1-s^2} \right).$$

Let $\mathbb{C}$ be the complex plane, and $\mathbb{C}^* = \mathbb{C} \setminus \{0\}$. For $z \in \mathbb{C}^*$, let g_1 and g_2 be transformations defined as

$$g_1(z) = ze^{\frac{2\pi}{n}i}, \tag{2}$$

$$g_2(z) = sze^{\frac{\pi}{n}i}, \tag{3}$$

where $i = \sqrt{-1}$. Recall the famous Euler formula $e^{i\theta} = \cos\theta + i\sin\theta$. It is obvious that g_1 represents a counter-clockwise rotation of $2\pi/n$ about the origin. The effect of g_2 is equivalent to a contraction of scale s first, and then followed by a counter-clockwise rotation of π/n about the origin. Geometrically, g_2 is equivalent to a counter-clockwise spiral contraction (thus $g_2^{-1}(z) = (1/s)ze^{-\frac{\pi}{n}i}$ is a clockwise spiral expansion). Denote the region of the tile $ABCD$ as Σ_0 and the symmetry group generated by g_1 and g_2 as $G(n,\alpha)$. Next, we investigate the effect of Σ_0 under group $G(n,\alpha)$.

In Fig.2(b), by the geometrical meaning of g_2, it is clear that $\Sigma_1 = g_2(\Sigma_0)$. In fact, by continuously applying g_2, we see that $\Sigma_k = g_2^k(\Sigma_0)$ for $k = 1, 2, 3, \ldots$. Thus, the set

$$\Sigma^* = \{\Sigma_k | \Sigma_k = g_2^k(\Sigma_0) \text{ for } k \in \mathbb{Z}\},$$

forms an infinite spiral arm. If we use g_1 to successively rotate the spiral arm Σ^* of $2\pi/n$ about the origin, we have

$$\begin{aligned}\mathbb{C}^* &= \{\Sigma^m | \Sigma^m = g_1^m(\Sigma^*) \text{ for } m = 1, 2, 3, \ldots, n\} \\ &= \sum_{m=1}^{n} \sum_{k=-\infty}^{+\infty} g_1^m[g_2^k(\Sigma_0)].\end{aligned} \tag{4}$$

Consequently, $G(n,\alpha)$ is a symmetry group of the rosette tiling and Σ_0 is a fundamental region associated with $G(n,\alpha)$. (4) gives a simple algorithm for constructing rosette tilings.

3 One-to-One Mapping Between Kite-Shaped and Square Regions

To embed a square image into tiles of a $G(n, \alpha)$ rosette tiling, in this section, we derive a one-to-one mapping between the kite-shaped region Σ_0 and the unit square.

For convenience, we set the origin of a new coordinate system $O'x'y'$ at the vertex D of tile Σ_0 (see Fig.3). Now, the tile $DABC$ is translated by a vector $(-s^2/(1-s^2), 0)$ to quadrilateral $O'A'B'C'$; Σ_0 is correspondingly denoted as Σ_0' (see Fig.3).

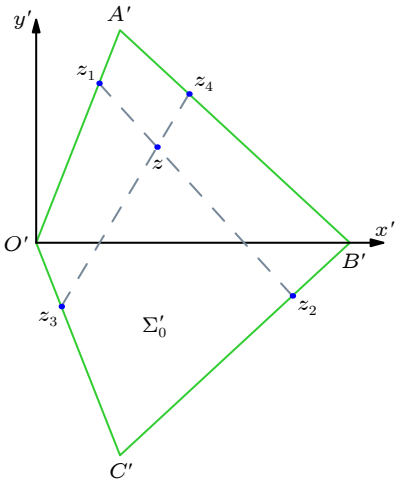

Fig.3. $z_1 \in O'A'$ and $z_3 \in O'C'$ are symmetrically placed boundary points of $z_2 \in B'C'$ and $z_4 \in A'B'$ that satisfy (5), respectively; point $z = x + yi \in \overline{z_1 z_2} \cap \overline{z_3 z_4}$.

In tile Σ_0', suppose $z_2 \in B'C'$ and $z_4 \in A'B'$ are symmetrically placed boundary points of $z_1 \in O'A'$ and $z_3 \in O'C'$, respectively. That is, z_k $(k = 1, 2, 3, 4)$ satisfy

$$\begin{aligned} z_2 + \frac{s^2}{1-s^2} &= g_2^{-1}\left(z_1 + \frac{s^2}{1-s^2}\right), \\ z_4 + \frac{s^2}{1-s^2} &= g_1\left(g_2^{-1}\left(z_3 + \frac{s^2}{1-s^2}\right)\right), \end{aligned} \tag{5}$$

where g_1 and g_2 are transformations defined in (2) and (3), respectively.

Denote the coordinates of A' as (a, b) and $\angle A'O'B' = \angle ADB = \phi$. It is easy to check that

$$\begin{aligned}(a,b) &= |O'A'|(\cos\phi, \sin\phi) \\ &= \frac{\cos(\frac{\pi}{2n} + \frac{\alpha}{2})}{\sin\alpha}(\cos\phi, \sin\phi),\end{aligned}$$

where $\phi = (n+1)\pi/2n - \alpha/2$. Assume that

$$\begin{aligned} z_1 &= vA', \\ z_2 - C' &= v(B' - C'), \end{aligned} \tag{6}$$

for $v \in [0, 1]$, and

$$\begin{aligned} z_3 &= uC', \\ z_4 - A' &= u(B' - A'), \end{aligned} \tag{7}$$

for $u \in [0, 1]$.

Let $z = x + yi$ be the intersection between segments $\overline{z_1z_2}$ and $\overline{z_3z_4}$, i.e., $z \in \overline{z_1z_2} \cap \overline{z_3z_4}$. We are going to map z onto a point (u, v) of the unit square (see Fig.4).

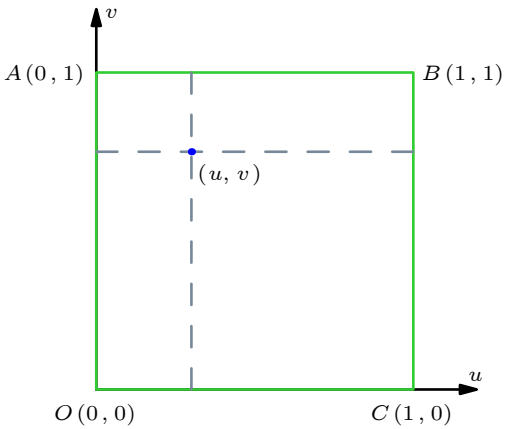

Fig.4. For a given point $z = x + yi \in \Sigma_0$ in Fig.3, (13) and (14) determine a unique point (u, v) in the unit square that corresponds to (x, y), where v and u are the roots of (13) and (14).

Note that $B' - C' - A' = (1 - 2a, 0)$ because $A' = (a, b)$, $B' = (1, 0)$, and $C' = (a, -b)$. By (6) and (7), we have

$$z_2 - z_1 = C' + v(1 - 2a, 0), \tag{8}$$

$$z_4 - z_3 = A' + u(1 - 2a, 0). \tag{9}$$

Let $z - z_1 = p_1(z_2 - z_1)$ for certain $p_1 \in [0, 1]$. By (6) and (8), we have

$$z = z_1 + p_1(z_2 - z_1) = vA' + p_1[C' + v(1 - 2a, 0)]. \tag{10}$$

Similarly, using (7) and (9), we can obtain

$$z = z_3 + p_2(z_4 - z_3) = uC' + p_2[A' + u(1 - 2a, 0)] \tag{11}$$

for certain $p_2 \in [0, 1]$.

By comparing the real and imaginary parts of (10), we get

$$\begin{cases} x = va + p_1a + p_1v(1 - 2a), \\ y = bv - b\,p_1. \end{cases} \tag{12}$$

By eliminating p_1 from (12), we derive a quadratic equation about v as

$$v^2(1 - 2a) + v\left(2a - \frac{y(1 - 2a)}{b}\right) - x - \frac{ay}{b} = 0. \tag{13}$$

With a similar treatment for (10), we obtain a quadratic equation about u from (11) as

$$u^2(1 - 2a) + u\left[2a + \frac{y(1 - 2a)}{b}\right] - x + \frac{ay}{b} = 0. \tag{14}$$

Given $z = x + yi \in \Sigma_0'$, by (13) and (14) we find a point $(u, v) \in [0,\ 1] \times [0,\ 1]$ (as the smaller roots in (13) and (14) are less than zero, we take the positive roots). This establishes a one-to-one mapping between Σ_0' and a square region so that we can embed a square image into the fundamental region Σ_0. Then, by (4), we can use copies of the image to construct a rosette drawing similar to "*Smaller and Smaller*".

4 Rendering of a Rosette Tiling

In this section, we introduce algorithms for rendering rosette tilings. All the algorithms rely on the algebraic structure of the tiling and the one-to-one mapping introduced in Section 2 and Section 3.

One way to render the rosette tiling is the direct use of (4). Thus, we take the fundamental region Σ_0, texture it using texture coordinates calculated using the one-to-one mapping in Section 3, and next, we use the generators g_1 and g_2 to obtain successive tiles of the tiling. Using (4), we generate the tiling of the whole space $\mathbb{C}$, but when we want to generate a rosette pattern like the one presented in Fig.2, in (4), we take only $k = 0,\ 1,\ 2,\ \ldots$.

Now, let us notice that

$$\begin{aligned} \Sigma_k &= g_2^k(\Sigma_0) = g_2(g_2^{k-1}(\Sigma_0)) \\ &= g_2(\Sigma_{k-1}), \quad k = 1,\ 2,\ \ldots, \\ \Sigma_k &= g_2^k(\Sigma_0) = g_2(g_2^{k+1}(\Sigma_0)) \\ &= g_2(\Sigma_{k+1}). \quad k = -1,\ -2,\ \ldots. \end{aligned}$$

These formulas show that a single spiral arm in the tiling is a simple feedback process. Therefore, we can use graphics card capabilities in the generation process, namely the transform feedback present in OpenGL and Vulkan.

The presented method is not the only method that we can use to render a rosette tiling. We can develop an algorithm that can be implemented in a fragment shader. From (4), we know that every point in the plane can be obtained by transforming some point from Σ_0 using g_1 and g_2. Thus, we need a method to, for a given $z \in \mathbb{C}$, find the corresponding point z' in Σ_0.

Firstly, let us examine the rosette tiling in Fig.5(a). We see that each area between two magenta lines contains the same pattern. Therefore, we can concentrate only on one such area because every point of the plane can be transformed to this area by a rotation using some multiple of $2\pi/n$ as the rotation angle, i.e., we use g_1^{-1} multiple times. In our method, we will select the area in which the argument of the points is between $-\pi/n$ and π/n (see the area be-

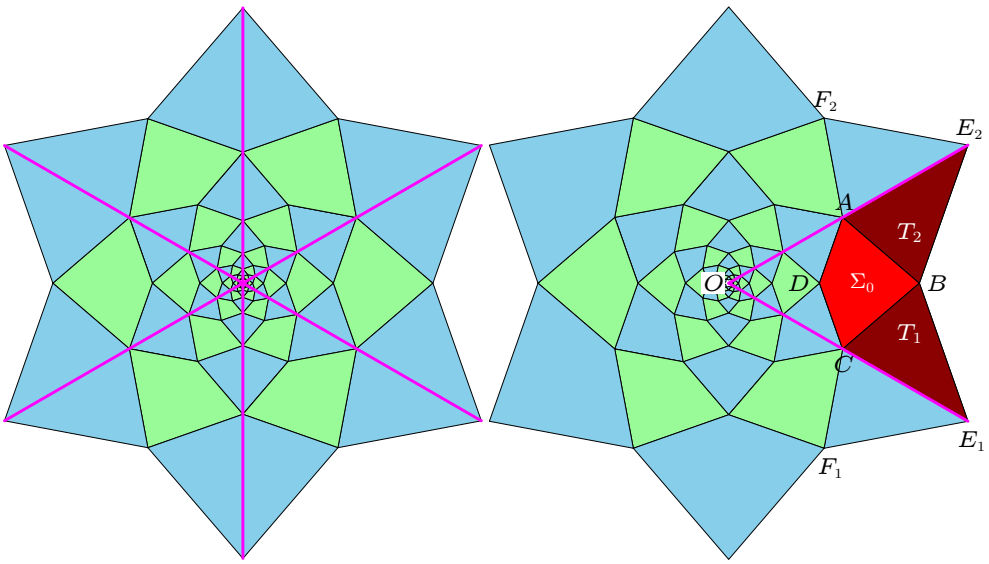

Fig.5. (a) Each area between two magenta lines of the rosette tiling contains the same pattern. (b) Every point between the two magenta lines can be transformed by scaling to one of the sets Σ_0, T_1, or T_2.

tween the magenta lines in Fig.5(b)). In this area, let us consider Σ_0 and the two triangles T_1 and T_2. The triangles are the halves of two kites of the tiling, i.e., the kites with the vertices B, C, F_1, E_1, and A, B, E_2, F_2. Therefore, the vertices E_1 and E_2 of the triangles can be calculated as follows:

$$\begin{aligned} E_1 &= g_2^{-1}(B), \\ E_2 &= g_1(g_2^{-1}(B)) = g_1(E_1). \end{aligned}$$

Now, let us consider the first green kite on the left of Σ_0 in Fig.5(b). We can transform it to Σ_0 by using

$$f_1(z) = g_2^{-1}(g_2^{-1}(g_1(z))) = \frac{1}{s^2}z.$$

We see that this is a scaling transformation with the scaling factor $1/s^2$. If we consider the second green kite to the left of Σ_0, then we can transform it to the first green tile using f_1 and then transform it to Σ_0 again using f_1. In general, we can gradually scale each green tile to the left of Σ_0 using f_1, and eventually, we reach Σ_0. Similar reasoning can be made for the blue triangles to the left of Σ_0, but this time the lower blue triangles are scaled using f_1 to T_1, and the upper ones to T_2. When we consider the kites to the right of Σ_0, we notice that we can repeat the same reasoning, but using

$$f_2(z) = g_1^{-1}(g_2(g_2(z))) = s^2 z,$$

which again is a scaling transformation, but with the scale factor s^2. Therefore, we can scale each point in the considered area to Σ_0, T_1 or T_2, i.e., the points inside the quad R with vertices C, B, A, O using the scaling factor $1/s^2$, and the scaling factor s^2 for the points outside of this quad. Of course, if we want to generate a rosette pattern like the one presented in Fig.2, then we only consider the points in R. The points outside of this quad are discarded.

Let z_s be the point after the scaling transformation. Now, we have three cases:

1) $z_s \in \Sigma_0$; therefore $z' = z_s$ and we solve (13) and (14) for z' to find the texture co-ordinates and texture z;

2) $z_s \in T_1$; therefore we transform it to Σ_0 using

$$z' = g_2(z_s),$$

and next, we solve (13) and (14) for z' to find the texture co-ordinates and texture z;

3) $z_s \in T_2$; therefore we transform it to Σ_0 using

$$z' = g_2(g_1^{-1}(z_s)),$$

and next, we solve (13) and (14) for z' to find the texture co-ordinates and texture z.

We summarize the method as pseudocode in Algorithm 1. In the algorithm, we assume that $\arg(z) \in [0, 2\pi)$.

5 Implementation and Gallery of Rosette Drawings in an Escher-Like Style

In this section, we specify some implementation details and give a gallery of the resulting Escher-like drawings.

Algorithm 1. Colour Calculation for a Rosette Tiling

Input: $z \in \mathbb{C}$: a point for which we calculate the colour; $n \in \mathbb{N}$, $\alpha \in [0, 2\pi]$: the parameters defining $G(n, \alpha)$; Σ_0: the fundamental region; T_1, T_2: triangles in Fig.5(b); s: the scaling factor in (1); g_1, g_2: generators of $G(n, \alpha)$; R: the quad with the vertices C, B, A, O (Fig.5(b)); b_{rosette}: a boolean variable, if true, then render the rosette pattern, else render the complete plane tiling; c_{bg}: background colour; T: a texture.

Output: Colour for z.

$m = \left\lfloor \dfrac{\arg(z) + (\pi/n)}{2\pi/n} \right\rfloor$
$z' = ze^{-m(2\pi/n)i}$
$s_f = 1/s^2$
if $z' \notin R$ **then**
  if b_{rosette} **then**
    return c_{bg}
  $s_f = s^2$
while $z' \notin \Sigma_0$ **and** $z' \notin T_1$ **and** $z' \notin T_2$ **do**
  $z' = s_f z$
if $z' \in T_1$ **then**
  $z' = g_2(z')$
else
  if $z' \in T_2$ **then**
    $z' = g_2(g_1^{-1}(z'))$
Find texture co-ordinates (u, v) for z' by solving (13) and (14)
return $T(u, v)$

Wallpaper groups allow both square, and diamond lattices[4, 5]. For a diamond wallpaper template, we need to transform it into a square template first. Fig.6 shows the process of producing a manta rosette drawing constructed from a wallpaper drawing of the diamond lattice. We first cut a diamond cycle template from Fig.6(a). Then we deform the template Fig.6(b) as the square template Fig.6(c), which can be realized by a simple affine transformation or a bilinear interpolation. Using the one-to-one mapping developed in Section 3, we next embed the square template Fig.6(c) into a kite-shaped region – the fundamental region associated with the rosette group. Finally, by (4), we use the kite-shaped template from Fig.6(d) to construct a rosette drawing. Fig.7 demonstrates the process of creating a rosette drawing constructed from a wallpaper pattern of a square lattice. For the square wallpaper template, except for the redundant step of converting the diamond template into a square template, all the other steps are similar to the diamond case. To save space, for the following cases, we will no longer display technical details, merely showing the deformed kite-shaped template at the upper right corner of each drawing.

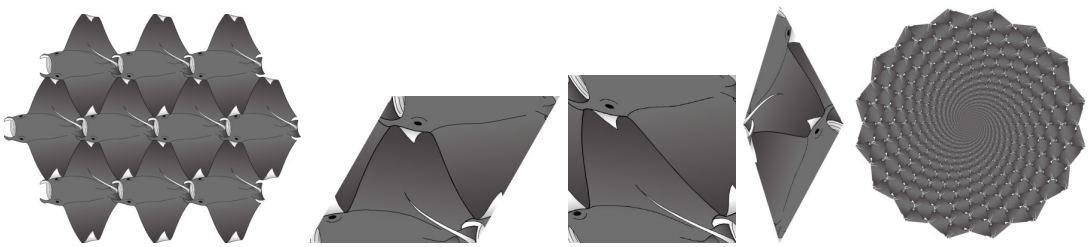

(a) (b) (c) (d) (e)

Fig.6. Process diagram of a rosette drawing constructed from a wallpaper drawing of diamond lattice. (a) A manta wallpaper drawing with a diamond lattice. (b) A cycle diamond template cut from (a). (c) The square template obtained by a bilinear interpolation of image (b). (d) Using the one-to-one correspondence given in (13) and (14), a kite-shaped template deformed from template (c). (e) A manta drawing constructed of $G(16, (45/360)2\pi)$ symmetry based on a kite-shaped template (d).

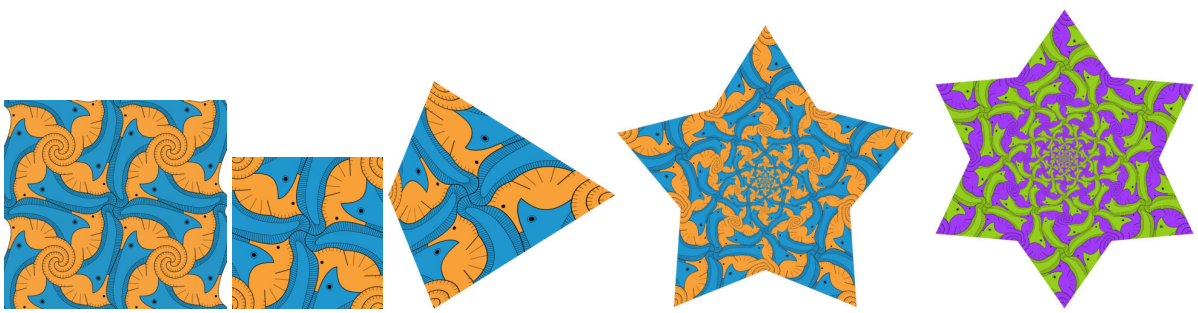

(a) (b) (c) (d) (e)

Fig.7. Process diagram of a rosette drawing constructed from a wallpaper drawing of square lattice. (a) A seahorse and eel drawing with square lattice. (b) A cycle square template cut from (a). (c) Using the one-to-one correspondence given in (13) and (14), a kite-shaped template deformed from template (b). (d) A seahorse and eel drawing of $G(5, (80/360)2\pi)$ symmetry constructed using the kite-shaped template (c). (e) By modifying colour data of template (b), we get a seahorse and eel drawing of $G(6, (80/360)2\pi))$ symmetry.

Using a strategy developed in [9] of modifying colours, Fig.7(e) displays a seahorse and eel drawing different from Fig.7(d). This approach can yield rich drawings of different styles easily and will be utilized in some of the next cases.

Rosette drawings demonstrated in Figs.7(d)–7(e) involve a technique called colour symmetry. Assuming S is a symmetry of template T, a colour symmetry of T is a permutation of colours which is compatible with S[5]. Intuitively, a colour symmetry template is a template in which colours of motifs are arranged symmetrically. Escher creatively introduced colour symmetry into his artworks, which greatly enhanced the aesthetic appeal[11]. Due to strong contrast, templates of colour symmetry would yield appealing drawings. Fig.8 and Figs.9(a)–9(d) display 10 rosette drawings of colour symmetry. The arrangement of template motifs may greatly affect the overall effect of rosette drawings. Figs.9(c)–9(d) illustrate a case in which the arrangements of the skate motifs differ a little. However, the resulting rosette drawings are quite different.

In Fig.9(e), we show a beetle rosette drawing of $G(13, (90/360)2\pi)$ symmetry. To obtain a better aesthetic effect, the boundary motifs are trimmed carefully so that a complete beetle is preserved. It should be pointed out that the square or diamond templates used in the construction of rosette drawings must satisfy periodic symmetries of wallpaper groups. Fig.9(f) shows a frog and crocodile rosette drawing of $G(12, (80/360)2\pi)$, which is a defective drawing since two halves of a crocodile at the edge of the template cannot form an intact normal crocodile motif. The fundamental reason is that the original square template does not meet the translational periodicity of wallpaper groups.

In 1958, Escher created a difficult artwork, *"Sphere Surface with Fish"* on the curved sphere space. In this work, the alternate rows of white and black fish spirally swim outwards from one pole to another; the fish attain the greatest size on the equator, and after that, they become smaller and disappear into poles. Now, we present a simple way to produce drawings similar to *"Sphere Surface with Fish"*.

Let $\boldsymbol{N} = (0,\ 0,\ 1) \in \mathbb{R}^3$ and let $\mathcal{S} = \{(x, y, z) \in \mathbb{R}^3 | x^2 + y^2 + z^2 = 1\}$ be the unit sphere in $\mathbb{R}^3$. The

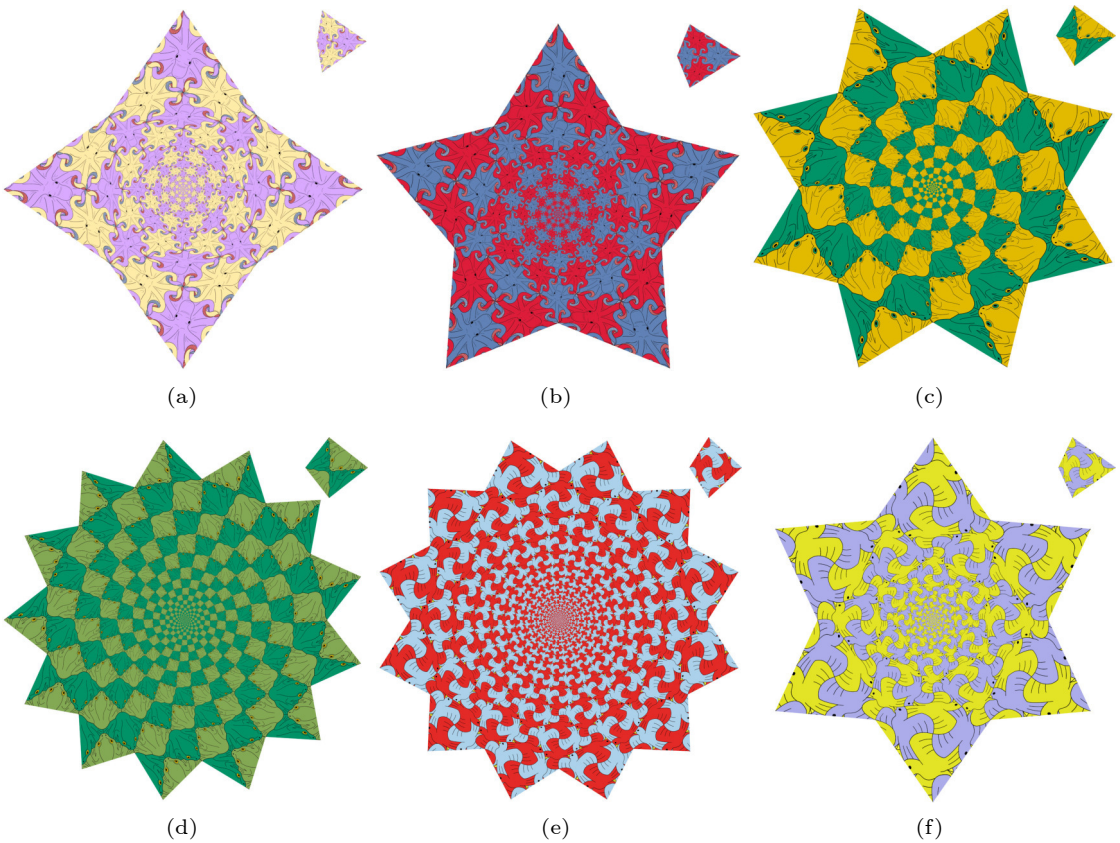

Fig.8. (a) An octopus drawing of $G(4, (65/360)2\pi)$ symmetry. (b) An octopus drawing of $G(5, (80/360)2\pi)$ symmetry. (c) A frog drawing of $G(8, (85/360)2\pi)$ symmetry. (d) A frog drawing of $G(13, (90/360)2\pi)$ symmetry. (e) A bird drawing of $G(12, (80/360)2\pi)$ symmetry. (f) A bird drawing of $G(6, (80/360)2\pi)$ symmetry.

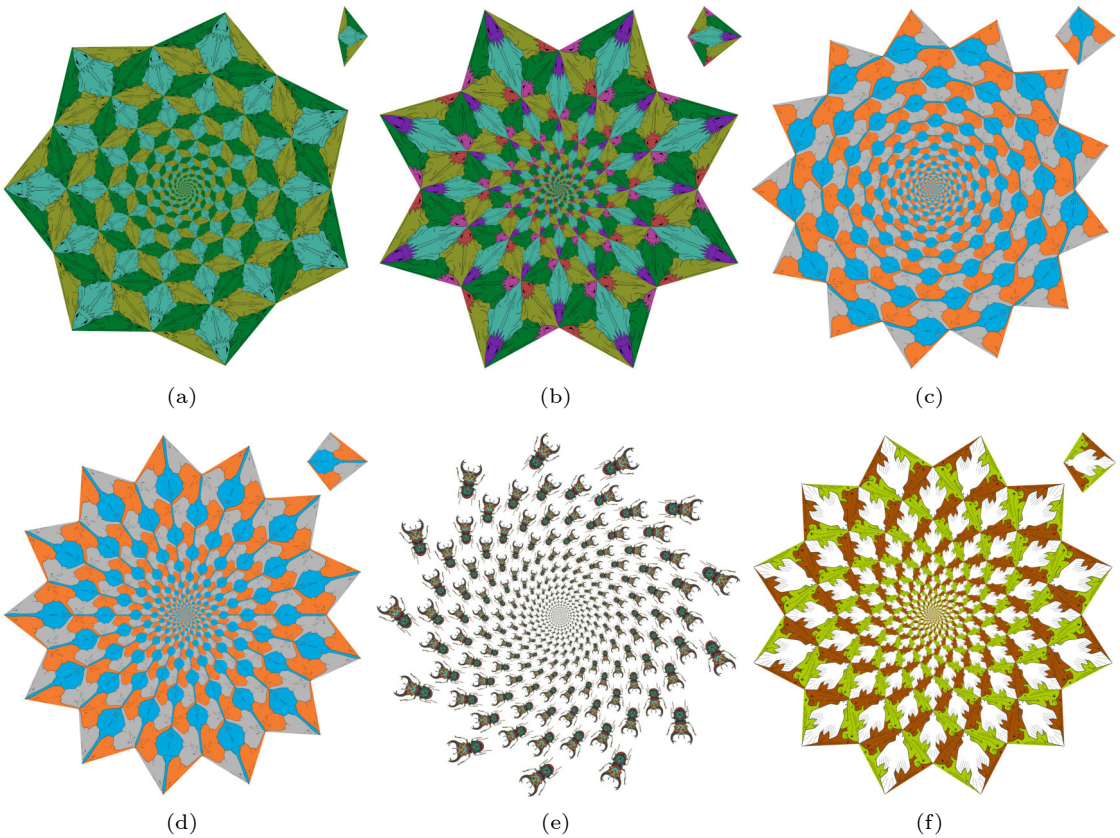

Fig.9. (a) A crocodile drawing of $G(7,(50/360)2\pi)$ symmetry. (b) A crocodile drawing of $G(8,(80/360)2\pi)$ symmetry. (c) A skate drawing of $G(13,(90/360)2\pi)$ symmetry. (d) A skate drawing of $G(13,(90/360)2\pi)$ symmetry. (e) A beetle drawing of $G(13,(90/360)2\pi)$ symmetry. (f) A defective frog and crocodile drawing of $G(12,(80/360)2\pi)$ symmetry.

stereographic projection of $\mathcal{S}$ to $\hat{\mathbb{C}}=\mathbb{C}\cup\{\infty\}$ from $\boldsymbol{N}$ is the map $\varphi:\mathcal{S}\to\hat{\mathbb{C}}$ given by the following formula

$$\varphi(x,y,z)=\begin{cases}\dfrac{x}{1-z}+\dfrac{y}{1-z}i, & \text{if } (x,y,z)\neq\boldsymbol{N},\\ \infty, & \text{if } (x,y,z)=\boldsymbol{N},\end{cases}$$

where $(x,y,z)\in\mathcal{S}$. The inverse map $\varphi^{-1}:\hat{\mathbb{C}}\to\mathcal{S}$ of φ is given by the formula

$$\varphi^{-1}(a+bi)=\begin{cases}\left(\dfrac{2a}{d},\dfrac{2b}{d},\dfrac{a^2+b^2-1}{d}\right), & \text{if } a+bi\in\mathbb{C},\\ \boldsymbol{N}, & \text{if } a+bi=\infty,\end{cases}$$

where $d=a^2+b^2+1$.

Now, suppose that P is a kite-based plane tiling. Then, by using φ^{-1} one can project P onto the finite sphere surface and obtain a spherical drawing. Fig.10 and Fig.11 show 12 spherical drawings similar to *"Sphere Surface with Fish"*.

6 Performance

To show the performance of the proposed rendering algorithm, we rendered the drawings in Fig.8(b) and Fig.9(c) of different resolutions. The drawing in Fig.8(b) has a low value of n, i.e., 5, whereas the drawing in Fig.9(c) was obtained for a higher value of n, i.e., 13. The rendering method was implemented in C++ using OpenGL and GLSL (OpenGL Shading Language). The computations were implemented in the fragment shader using double precision numbers. Moreover, we rendered the drawings without anti-aliasing, i.e., one sample per pixel, and with anti-aliasing using multi-sampling with various numbers of samples per pixel (2, 4, and 8). The tests were performed on a computer with the following specifications: NVIDIA GeForce GTX 1 660 Ti graphics card with 6 GB GDDR6 SDRAM, Intel i5-9600K (@3.70 GHz), 32 GB DDR4 RAM and Windows 10 (64 bit).

The resultant rendering time (in milliseconds) are gathered in Table 1 for Fig.8(b), and in Table 2 for Fig.9(c). For both drawings, we see that the generation time in the case of one sample per pixel (no anti-aliasing) is very short. For low resolution ($1\,000\times1\,000$ pixels), it is equal to 8 ms–9 ms, and for high resolution ($8\,000\times8\,000$ pixels), between 300 and 400 milliseconds. When we turn the anti-aliasing

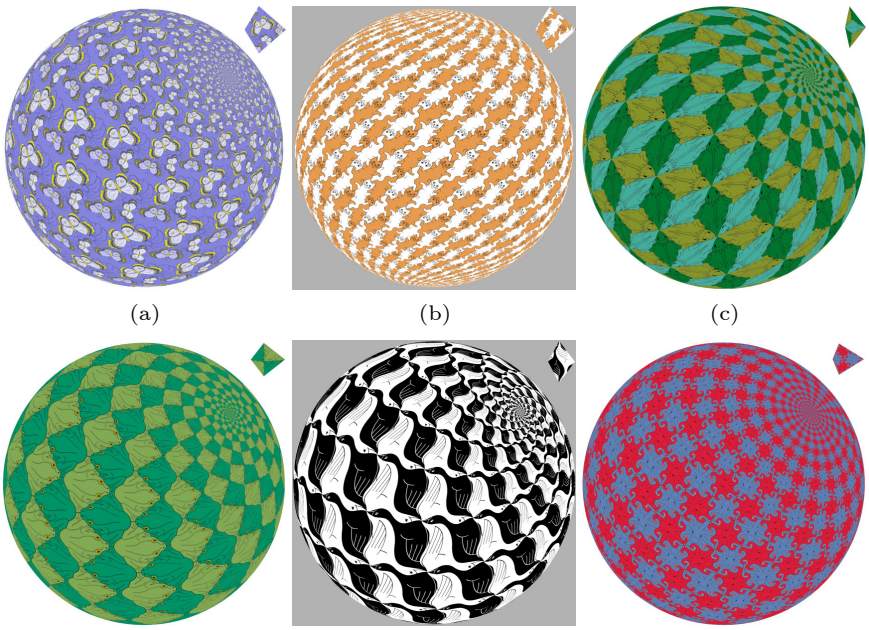

Fig.10. (a) A spherical butterfly drawing of $G(10, (80/360)2\pi)$ symmetry. (b) A spherical cat drawing of $G(12, (80/360)2\pi)$ symmetry. (c) A spherical crocodile drawing of $G(10, (55/360)2\pi)$ symmetry. (d) A spherical frog drawing of $G(9, (85/360)2\pi)$ symmetry. (e) A spherical goose drawing of $G(19, (65/360)2\pi)$ symmetry. (f) A spherical octopus drawing of $G(10, (75/360)2\pi)$ symmetry.

on, then the time is longer, but the quality of the generated drawings is greater, especially in the areas where many tiny details appear. For two samples per pixel, we observe time is less than a second, even for high resolutions. For four and eight samples per pixel, only for the resolution of $8\,000 \times 8\,000$ pixels, we get time longer than one second, i.e., for four samples, the time is longer than two seconds, whereas, for eight samples, the time is longer than three seconds.

The proposed rendering method of rosette drawings has also low memory requirements. We only need memory for the rendered image and several variables needed in the calculations.

7 Conclusions

Inspired by Escher's *"Smaller and Smaller"*, this paper considered the computer-aided generation of Escher-like rosette drawings. We first introduced the symmetry group to analyze the geometrical structure of rosette tilings. Then, to embed a pre-designed template into kite-shaped tiles of a rosette tiling, we elaborated a one-to-one mapping between the kite-shaped and square regions. We finally specified some implementations of drawings similar to *"Smaller and Smaller"* and *"Sphere Surface with Fish"*. The proposed method can create rich drawings using existing wallpaper templates.

The kite-based tilings obtained with the proposed method are generated directly without using any non-linear mapping. They can be controlled in a natural way using the two parameters of the symmetry group $G(n, \alpha)$. Moreover, we can design the motif in a square texture without the need to take into account any non-linear mappings. The embedding of the texture into the kite is easy and fast because we solve simple quadratic equation. Therefore, the proposed method eliminates all the drawbacks of the method based on the anti-Mercator mapping mentioned in the introduction.

In contrast to the methods reported in [21, 22][⑦, ⑧, ⑨, ⑩, ⑪], the approach developed in this paper has several advantages. First, the construction of rosette tilings merely involves simple similarity and rotation transformations, which makes the resulting drawings present a strong spiral effect (because tiles

⑦https://tessellations.ca/2017/05/04/deforming-your-tessellations-into-infinite-spirals/, Nov. 2024.
⑧https://apps.apple.com/us/app/id534529876?platform=ipad, Nov. 2024.
⑨https://www.tissellator.com/, Nov. 2024.
⑩https://isohedral.ca/escher-like-spiral-tilings/, Nov. 2024.
⑪http://www.josleys.com/show_gallery.php?galid=290, Nov. 2024.

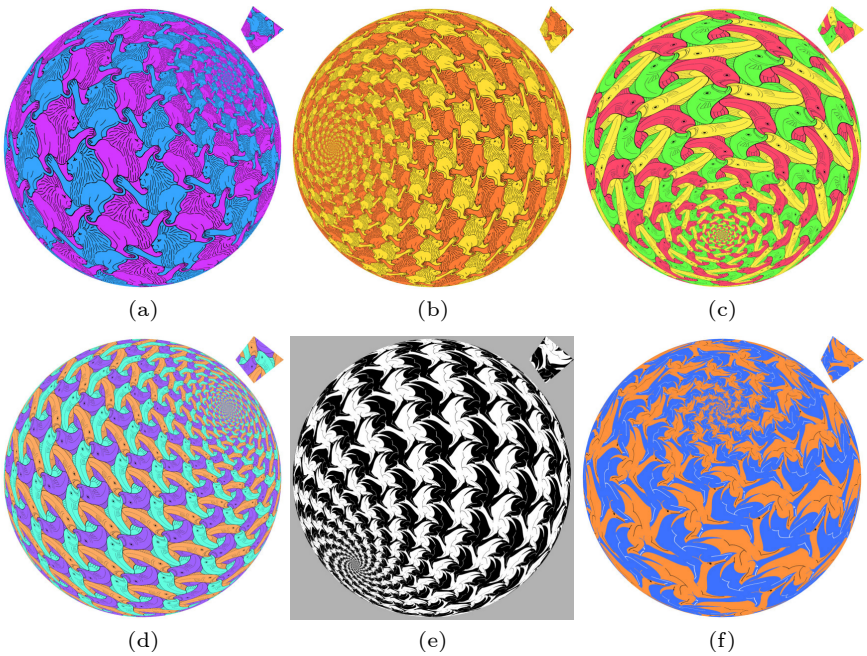

Fig.11. (a) A spherical lion drawing of $G(7,(80/360)2\pi)$ symmetry. (b) A spherical lion drawing of $G(10,(35/360)2\pi)$ symmetry. (c) A spherical fish drawing of $G(8,(85/360)2\pi)$ symmetry. (d) A spherical fish drawing of $G(13,(90/360)2\pi)$ symmetry. (e) A spherical dragon drawing of $G(12,(85/360)2\pi)$ symmetry. (f) A spherical dragon drawing of $G(7,(80/360)2\pi)$ symmetry.

Table 1. Rendering Time (ms) of Fig.8(b) Using the Proposed Rendering Algorithm for Various Resolutions (in Pixels) and Number of Samples

Resolution	One Sample	Two Samples	Four Samples	Eight Samples
1 000 × 1 000	8.517	16.803	33.667	61.350
2 000 × 2 000	33.118	65.239	116.338	202.251
4 000 × 4 000	129.299	203.397	327.665	566.856
8 000 × 8 000	327.971	551.430	2 056.120	3 020.710

Table 2. Rendering Time (ms) of Fig.9(c) Using the Proposed Rendering Algorithm for Various Resolutions (in Pixels) and Number of Samples

Resolution	One Sample	Two Samples	Four Samples	Eight Samples
1 000 × 1 000	9.526	19.105	35.173	67.047
2 000 × 2 000	36.224	68.214	131.132	215.955
4 000 × 4 000	136.665	218.860	376.312	728.326
8 000 × 8 000	381.989	703.412	2 359.940	3 646.360

have no distortion). It also provides an easy-to-implement measure to design spiral patterns by hand (see a case demonstrated in Figs.12(a)–12(b)). Second, our method is straightforward and elementary. We did not introduce complex functions that cannot be easily understood by ordinary people (such as the anti-Mercator mapping used by Kaplan[10]). Finally, based on computer graphic technology, we developed a mathematical algorithm to obtain Escher-like drawings. The precise mathematical approach completely avoids the human errors inherent in Escher's manual creative process.

The applications of Escher-like rosette drawings span across at least five domains, demonstrating the versatility and practical utility of the proposed methods.

Textile Design. The techniques enable the creation of unique, symmetrical patterns for textiles in fashion and home decor. This allows designers to produce distinctive fabric prints that enhance the visual appeal of clothing and interior fabrics, such as curtains and upholstery.

Interior Decoration. The generated patterns can be utilized in designing wallpapers, floor tiles, and

[10] https://isohedral.ca/escher-like-spiral-tilings/, Nov. 2024.

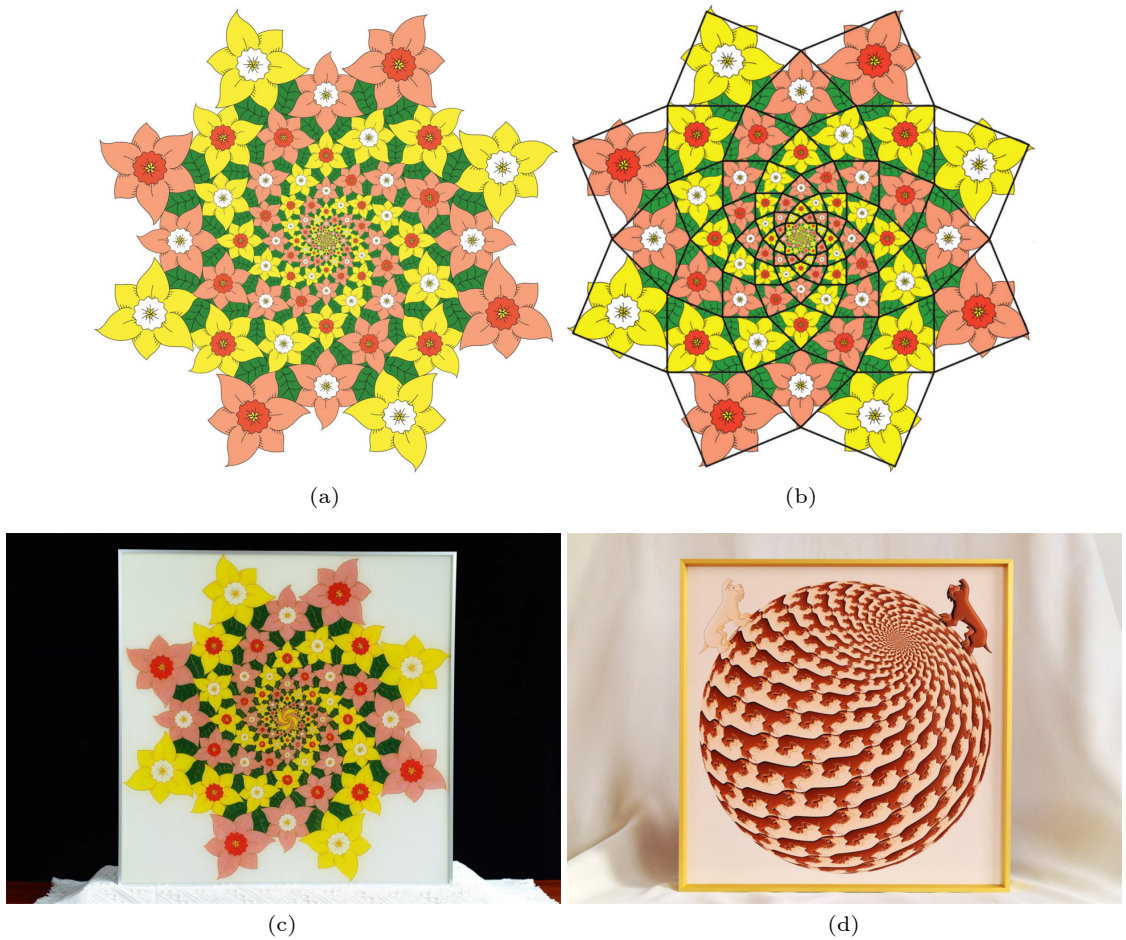

Fig.12. (a) An Escher-like follower drawing by the third author of the paper obtained with the help of Adobe Illustrator. (b) The Escher-like follower drawing from (a) emphasized with a rosette tiling. (c) A manual cloisonne handicraft (65 cm × 65 cm) based on (b). (d) A Jingdezhen high-temperature porcelain (45 cm × 45 cm) based on an Escher-like spherical dog drawing.

furniture coverings. These applications help in achieving aesthetically pleasing and thematic interior spaces, tailored to specific styles or colour schemes.

Poster and Graphic Design. In the realm of advertising and marketing, these complex patterns can be incorporated into posters, flyers, and digital advertisements. They serve as eye-catching elements that can effectively capture attention and convey messages, thereby enhancing brand recognition and visual impact.

Digital Media and Web Design. The patterns can be applied to digital interfaces, including websites and virtual reality environments, to create engaging visual experiences. They add depth and interest to digital backgrounds and elements, improving user interaction and overall digital aesthetics.

Educational Tools. These patterns also serve an educational purpose by illustrating mathematical concepts such as symmetry, geometry, and tessellation. They can be integrated into educational materials to make learning these concepts more engaging and visually intuitive for students.

Overall, the broad applicability of these Escher-like patterns underscores their potential to influence diverse fields. This not only benefits the aesthetic and functional aspects of products and spaces but also enhances the educational approaches in understanding complex mathematical principles. In the future, we plan to generate richer Escher-like tessellations and explore the commercial potential of Escher artwork (see two examples shown in Figs.12(c)–12(d)).

Conflict of Interest The authors declare that they have no conflict of interest.

References

[1] Barnsley M F. Fractals Everywhere (3rd edition). Dover Publications, 2012.

[2] Gdawiec K. Inversion fractals and iteration processes in the generation of aesthetic patterns. *Computer Graphics*

Forum, 2017, 36(1): 35–45. DOI: 10.1111/cgf.12783.

[3] Field M, Golubitsky M. Symmetry in Chaos: A Search for Pattern in Mathematics, Art, and Nature (2nd edition). Society for Industrial and Applied Mathematics, 2009.

[4] Carter N C, Eagles R L, Grimes S M, Hahn A C, Reiter C A. Chaotic attractors with discrete planar symmetries. *Chaos, Solitons & Fractals*, 1998, 9(12): 2031–2054. DOI: 10.1016/S0960-0779(97)00157-4.

[5] Grünbaum B, Shephard G C. Tilings and Patterns (2nd edition). Dover Publications, 2016.

[6] Zou Y, Li W, Lu J, Ye R. Orbit trap rendering method for generating artistic images with cyclic or dihedral symmetry. *Computers & Graphics*, 2006, 30(3): 470–473. DOI: 10.1016/j.cag.2006.02.009.

[7] Dunham D, Lindgren J, Witte D. Creating repeating hyperbolic patterns. *ACM SIGGRAPH Computer Graphics*, 1981, 15(3): 215–223. DOI: 10.1145/965161.806808.

[8] Ouyang P, Chung K. Beautiful math, part 3: Hyperbolic aesthetic patterns based on conformal mappings. *IEEE Computer Graphics and Applications*, 2014, 34(2): 72–79. DOI: 10.1109/MCG.2014.23.

[9] Ouyang P C, Tang X, Chung K W, Yu T. Spiral patterns of color symmetry from dynamics. *Nonlinear Dynamics*, 2018, 94(1): 261–272. DOI: 10.1007/s11071-018-4357-0.

[10] Stock D L, Wichmann B A. Odd spiral tilings. *Mathematics Magazine*, 2000, 73(5): 339–346. DOI: 10.1080/0025570X.2000.11996873.

[11] Schattschneider D. M. C. Escher: Visions of Symmetry. Harry N. Abrams, 2004.

[12] Kaplan C S. Computer graphics and geometric ornamental design [Ph. D. Thesis]. University of Washington, Washington, 2002.

[13] Kaplan C S, Salesin D H. Escherization. In *Proc. the 27th Annual Conference on Computer Graphics and Interactive Techniques*, Jul. 2000, pp.499–510. DOI: 10.1145/344779.345022.

[14] Yen J, Séquin C. Escher sphere construction kit. In *Proc. the 2001 Symposium on Interactive 3D Graphics*, Mar. 2001, pp.95–98. DOI: 10.1145/364338.364371.

[15] Kaplan C S. Metamorphosis in Escher's art. In *Bridges Leeuwarden: Mathematics, Music, Art, Architecture, Culture*, Sarhangi R, Séquin C H (eds.), Tarquin Publications, 2008, pp.39–46.

[16] Ouyang P C, Chung K W, Nicolas A, Gdawiec K. Self-similar fractal drawings inspired by M. C. Escher's print Square Limit. *ACM Trans. Graphics*, 2021, 40(3): 31. DOI: 10.1145/3456298.

[17] Lin S S, Morace C C, Lin C H, Hsu L F, Lee T Y. Generation of Escher arts with dual perception. *IEEE Trans. Visualization and Computer Graphics*, 2018, 24(2): 1103–1113. DOI: 10.1109/TVCG.2017.2660488.

[18] Sugihara K. Computer-aided generation of Escher-like Sky and Water tiling patterns. *Journal of Mathematics and the Arts*, 2009, 3(4): 195–207. DOI: 10.1080/17513470903185626.

[19] Ouyang P C, Fathauer R W, Chung K W, Wang X. Automatic generation of hyperbolic drawings. *Applied Mathematics and Computation*, 2019, 347:653–663. DOI: 10.1016/j.amc.2018.09.052.

[20] von Gagern M, Richter-Gebert J. Hyperbolization of Euclidean ornaments. *The Electronic Journal of Combinatorics*, 2009, 16(2): #R12. DOI: 10.37236/78.

[21] Dixon R. Two conformal mappings. *Leonardo*, 1992, 25(3/4): 263–266. DOI: 10.2307/1575848.

[22] Marcotte J, Salomone M. Loxodromic spirals in M. C. Escher's Sphere Surface. *Journal of Humanistic Mathematics*, 2014, 4(2): 25–46. DOI: 10.5642/jhummath.201402.04.

[23] Fathauer R. Art and recreational math based on kite-tiling rosettes. In *Proceedings of Bridges 2018: Mathematics, Art, Music, Architecture, Education, Culture*, Torrence E, Torrence B, Séquin C, Fenyvesi K (eds.), Tessellations Publishing, 2018, pp.15–22.

[24] Fathauer R. Tessellations: Mathematics, Art, and Recreation. CRC Press, 2021.

Pei-Chang Ouyang is currently a professor at the School of Science, Guangxi University of Science and Technology, Liuzhou. He received his Ph.D. degree in 2012 from Sun Yat-Sen University, Guangzhou. His research interests include fractals, tilings, computer graphics, and the generation of Escher-like patterns.

Kwok-Wai Chung is a retired associate professor at the Department of Mathematics, City University of Hong Kong, Hong Kong. He received his Ph.D. degree in 1989 from University of York, UK. His research interests include dynamical systems, bifurcation, chaos, and the generation of Escher-like patterns.

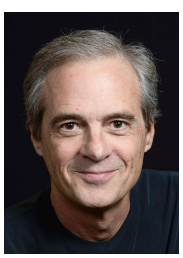

Robert W. Fathauer is the owner of a small business producing polyhedral dice, tessellation puzzles, and related products. He received his Ph.D. degree from Cornell University in electrical engineering and has been making art incorporating mathematics for over 30 years. He has written numerous papers on his explorations in recreational mathematics.

Alain Nicolas is one of the best designers of Escher-like arts, the first artist to make tilings with words and make aperiodic figurative tilings (http://en.tessellations-nicolas.com/). To propose a better adapted method for creating Escher-like arts, he published his French book *Parcelles d'infini* in 2005 at the Belin Pour la Science library.

Jian-Hua Pang is currently a professor at the School of Science, Guangxi University of Science and Technology, Liuzhou. She received her Ph.D. degree in 2012 from Nanjing Normal University, Nanjing. Her research interests include computer graphics, mathematical models, and the generation of Escher-like patterns.

Shi-Yun Cao is currently an assistant professor at the School of Science, Guangxi University of Science and Technology, Liuzhou. His research interests include complex data analysis, machine learning, and computer graphics.

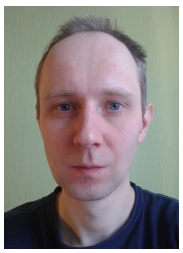

Krzysztof Gdawiec received his M.Sc. degree in mathematics from University of Silesia, Poland, in 2005, his Ph.D. degree in computer science from the same university in 2010, and his D.Sc. degree in computer science from the Warsaw University of Technology, Poland, in 2018. He is currently employed as an associate professor at the Institute of Computer Science of the University of Silesia. His main research interests include computer graphics, applications of fractal geometry, game development, and the generation of Escher-like patterns. He is a member of the Polish Mathematical Society and SIGGRAPH.